# MICROSCOPIC DESCRIPTION OF SUPERHEAVY NUCLEI WITH THE GOGNY EFFECTIVE INTERACTION

J.F. Berger, D. Hirata and M. Girod

Service de Physique Nucléaire, CEA-Bruyères-le-Châtel
BP 12, 91680 Bruyères-le-Châtel, France

*(Received October 28, 2002)*

*Dedicated to Adam Sobiczewski in honour of his 70th birthday*

An overview of the structure and stability properties of superheavy nuclei obtained from a microscopic approach employing the Gogny effective nucleon–nucleon interaction is presented. Shell gaps, fission barriers and stability against $\alpha$-decay are discussed and compared with experimental data and other theoretical approaches. In particular, a few $\alpha$-decay chains of odd nuclides observed in recent experiments are examined.

PACS numbers: 21.10, 21.60, 27.90.+b, 23.60.+e

## 1. Introduction

The theoretical description of superheavy (SHE) nuclei represents a very stringent test of nuclear structure models. Internal structure effects, such as shells and pairing correlations are essential for explaining the stability properties of nuclei beyond $Z \simeq 100$. Apart from preventing these nuclei from instantaneous spontaneous fission, they strongly influence the heights of fission barriers and the probabilities of various kinds of particle decay. In this context, the progress made in recent years in the synthesis of very heavy nuclides at several experimental facilities over the world [1–4] has been of considerable help for guiding theoretical work. For instance, shell-stabilised deformed SHE in the $Z = 108$ region [5, 6] have been produced. Element $Z = 112$ has been discovered first at GSI [7], then in Dubna where one isotope of element 114 has also been found [8]. Last year, the identification of $^{292}116$ has been reported and the decay chains of the previously observed $^{288}114$ have been confirmed [9].

On the theoretical side, predictions concerning the stability of transactinide nuclei have been proposed since many years. Many of them use the macroscopic–microscopic method based on the Strutinski shell correction technique [10] and an impressive body of results has been derived concerning masses, spectra and lifetimes [11–16]. In recent years, this method has evolved into an approach of considerable sophistication [12, 13, 17] whose results often are in excellent agreement with experimental data. In this context, the Warsaw school has played a very influential role, participating in the first works in the domain of superheavy nuclei [18] and proposing a number of predictions concerning their properties [12]. One of the most important of them has been the discovery that deformed shell closures existed around nucleon numbers $N = 162$ and $Z = 108$ [17].

In the last ten years, an increasing number of calculations devoted to transactinide nuclei have been made in the framework of microscopic approaches. They are usually based on the full Hartree–Fock–Bogolyubov (HFB) procedure [19], where both the average field and the pairing field are derived self-consistently from an effective nucleon–nucleon interaction. Calculations using contact forces such as Skyrme interactions to compute the nuclear mean-field must employ a different interaction in the pairing channel. In contrast, HFB calculations with the finite range Gogny force use the same interaction in both channels. The advantage of a microscopic approach is to treat on the same footing bulk — liquid-drop like — effects and quantal effects arising from shells and pairing. In addition, the functional form of the nuclear average field is not *a priori* prescribed. Such features can be important for very heavy nuclei where high order multipole deformations can develop, in particular along fission barriers [20]. On the other hand, the interpretation of results obtained from HFB calculations may be delicate since effects coming from correlations beyond the mean-field approximation can be important. For instance, single particle energies in principle should be renormalized due to the coupling of nucleon propagation to oscillations of the mean field, which can affect the location and magnitude of magic nucleon numbers in the superheavy region. Moreover, they are indications that such effects depend on the kind of effective interaction employed.

The purpose of this paper is to present an overview of the structure and stability properties in superheavy elements deduced from a microscopic approach employing the Gogny effective interaction [21]. The set of parameters called D1S [22] is used. Extensive applications have shown that this parametrization of the effective interaction is able to describe a broad range of nuclear phenomena in nuclei from the lighter ones up to actinides [21,23]. In this context, the microscopic analysis of superheavy nuclei discussed here can be viewed both as a test of the validity of this interaction for large nucleon numbers and as an attempt to make predictions in this rich domain.

A brief presentation of theoretical methods is given in Sec. 2. Sec. 3 describes the results obtained with this approach concerning shell gaps, fission barriers and lifetimes with respect to $\alpha$-decay for nuclei ranging between $Z = 104$ and $Z = 128$. Some of the results shown here have already appeared previously [24]. Among new ones, let us mention calculations of $\alpha$-decay energies in a few chains of odd nuclides which have been measured in recent experiments.

## 2. The microscopic approach

The basis of our microscopic approach is the Hartree–Fock–Bogoliubov (HFB) theory. The effective nuclear Hamiltonian is assumed to be

$$H = \sum_{\alpha,\beta} T_{\alpha\beta}\, c^\dagger_\alpha c_\beta + \frac{1}{4} \sum_{\alpha,\beta,\gamma,\delta} v_{\alpha\beta\gamma\delta}\, c^\dagger_\alpha c^\dagger_\beta c_\delta c_\gamma \,, \tag{1}$$

where $c^\dagger_\alpha$ and $c_\alpha$ are creation and annihilation operators associated with a complete representation of single particle nuclear states $|\alpha\rangle$, $T_{\alpha\beta}$ are matrix elements of the kinetic energy in this representation, and $v_{\alpha\beta\gamma\delta}$ are the antisymmetrised matrix elements of the two-body interaction.

In the case of even–even nuclei the HFB equations are derived by applying a variational principle to the mean-value of the Hamiltonian (1) in a state $|\tilde{0}\rangle$ which is assumed to be the vacuum of quasiparticles operators of the form

$$\eta^\dagger_\mu = \sum_\alpha (U_{\mu\alpha}\, c^\dagger_\alpha + V_{\mu\alpha}\, c_\alpha) \,. \tag{2}$$

In odd nuclei, use is made of the blocking technique, *i.e.* the trial state $|\tilde{0}\rangle$ is replaced by $\eta^\dagger_{\mu_b}|\tilde{0}\rangle$, where $\mu_b$ labels the quasi-particle state chosen to represent the odd nucleon orbital. In the present work, time-reversal symmetry of the mean-field and pairing fields is preserved by taking averages over the nuclear state $\eta^\dagger_{\mu_b}|\tilde{0}\rangle$ and its time-reversed $\eta^\dagger_{\overline{\mu_b}}|\tilde{0}\rangle$. The ground state and low-lying excited states of the nucleus are then obtained by performing successive HFB calculations with different $\mu_b$.

The constraints $\langle\tilde{0}|\hat{N}|\tilde{0}\rangle = N$ and $\langle\tilde{0}|\hat{Z}|\tilde{0}\rangle = Z$ ensuring that $|\tilde{0}\rangle$ describes a nucleus having on the average $N$ neutrons and $Z$ protons are taken care of by adding $-\mu_n\hat{N} - \mu_p\hat{Z}$ to $H$, where $\mu_n$ and $\mu_p$ are Lagrange parameters representing the neutron and proton chemical potentials. The $U$ and $V$ in (2) are then found to be the solutions of the HFB system of equations

$$\sum_\gamma \begin{pmatrix} h_{\alpha\gamma} - \mu_{\tau_\alpha}\delta_{\alpha\gamma} & \Delta_{\alpha\gamma} \\ -\Delta^*_{\alpha\gamma} & -h^*_{\alpha\gamma} + \mu_{\tau_\alpha}\delta_{\alpha\gamma} \end{pmatrix} \begin{pmatrix} U_\gamma \\ V_\gamma \end{pmatrix} = \epsilon_\alpha \begin{pmatrix} U_\alpha \\ V_\alpha \end{pmatrix}, \tag{3}$$

where $h$ is the matrix of the one-body Hartree–Fock Hamiltonian, the sum of the kinetic energy and of the nuclear average field, and $\Delta$ is the matrix of the pairing field.

In order to derive potential energy surfaces (PES), multipole constraints $\langle\tilde{0}|\hat{Q}_{lm}|\tilde{0}\rangle = Q_{lm}$ are introduced. This is done by adding to $H$ external fields $-\lambda_{lm}\hat{Q}_{lm}$ allowing one to vary different kinds of nuclear multipole deformations. Let us note that multipole deformations not subject to explicit constraints automatically adopt the values that minimize the total deformation energy.

The results presented in the next section have been obtained by using the D1S interaction proposed by Gogny [21,22]. This is a finite range interaction which has been designed in order to describe simultaneously the nuclear mean-field and pairing correlations. Non-local effects in the average field (exchange terms) as well as all multipoles of the pairing field are taken into account. Concerning the Coulomb field between protons, the direct contribution is computed exactly, whereas the Slater approximation is used in the exchange term. One- and two-body corrections for center of mass motion are extracted self-consistently.

The constrained HFB equations are solved by expanding quasi-particle states on finite sets of deformed harmonic oscillator states containing at least 15 major shells. In most of the calculations presented here, axial symmetry is assumed and a constraint on the axial quadrupole moment $Q_{20}$ is used. However, single quasi-particle states are not required to have good parity. Consequently, the effect of a spontaneous breaking of the left–right symmetry of the nuclear shape can be analyzed, in particular on fission barriers. In a few instances, calculations have been performed in triaxial symmetry. In these cases, a constraint on the non-axial quadrupole moment $Q_{22}$ associated with $\gamma$ deformation is introduced, and only left–right symmetric shapes are envisaged [25].

Moments of inertia and an inertia tensor for multipole vibrations are computed as functions of the deformation parameters by means of formulas of the Inglis–Belyaev type [26]. Inertia and PES can then be used to build a quantized collective Hamiltonian, whose diagonalisation yields eigenenergies and collective wave functions describing a correlated ground state and vibrational excitations [27]. With this method, zero-point energies in ground state and isomeric wells can be computed, as well as ground state "dynamical" $\beta$-deformations including the effect of quadrupole oscillations. The computed inertia and PES can also be used to estimate spontaneous fission lifetimes within the standard WKB approximation [28]. $Q_\alpha$ are calculated from mass differences including the above mentioned zero-point energies. Half-lives $T_{1/2}(\alpha)$ are then derived from an empirical model [29] depending on 9 parameters which have been determined in order to reproduce experimental $\alpha$-decay lifetimes of even–even $\alpha$-emitters in the rare-earth and actinide regions.

## 3. Results and discussion

### *3.1. Shells*

As mentioned in the introduction, the stability of transactinide nuclei strongly depends on their internal structure, in particular on the presence of gaps in single-particle spectra. Fig. 1 shows the magnitude of the neutron Fermi gap obtained at sphericity with the Gogny force in $N = 184$ isotones from $Z = 110$ to $Z = 128$ (left part), and the spherical proton Fermi gaps in several $Z = 114$, $Z = 120$ and $Z = 126$ isotopes (right part). In all $N = 184$ isotones, the gap is of the order of 3 MeV, with a slight increase in the vicinity of $Z = 126$. A strongly different pattern appears on the proton side: proton shell gaps are found smaller and they significantly depend on neutron number. From this figure, the "best" doubly magic superheavy nuclei are $^{310}126_{184}$ and, to a lesser extent, $^{292}120_{172}$. The first of these two nuclei is found to be a rigid spherical nucleus bearing resemblance with $^{208}$Pb, whereas the second one adopts the form a "semi-bubble", *i.e.* the nucleon density at the centre of the nucleus is only two thirds of the normal density [30].

One observes that $Z = 114$ is not really a magic number, contrary to the predictions of most macroscopic–microscopic methods [12, 13, 31]. For instance, proton pairing correlations contribute 17 MeV to the binding energy

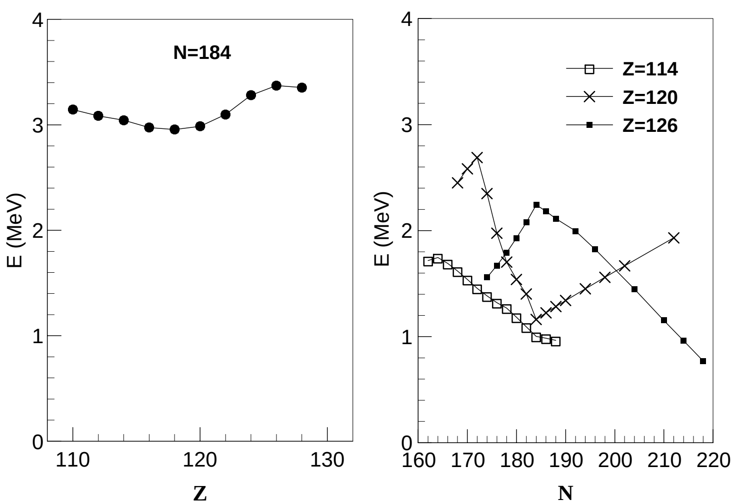


Fig. 1. Left: Spherical Fermi gap for neutrons in ten $N = 184$ isotones. Right: Spherical Fermi gaps for protons in several $Z = 114$, 120 and 126 isotopes.

of $^{298}114_{184}$. However, as in macroscopic–microscopic calculations, a spherical neutron subshell is found at $N = 164$ with the Gogny force and a proton one at $Z = 92$ (see Fig. 2). One can say that neutron and proton spherical shells are the same in the two approaches except that $Z = 114$ is replaced with $Z = 126$. Let us add that the magic number we obtain next to $N = 184$ is $N = 228$.

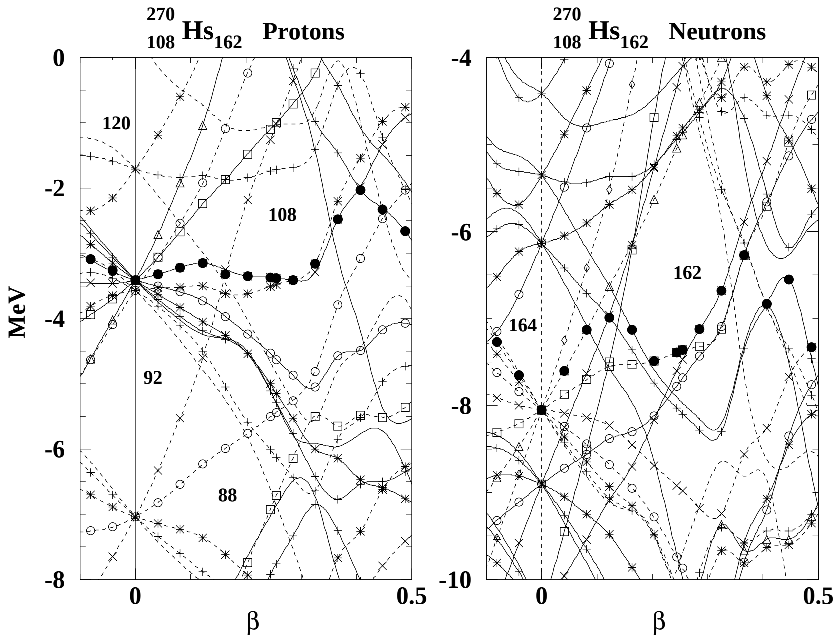


Fig. 2. Proton and neutron single particle energies in the vicinity of the Fermi surface in $^{270}$Hs as functions of axial quadrupole deformation. Values of $j_z$ from 1/2 to 15/2 are indicated by dots, $+$, $*$, circles, $\times$, squares, triangles, diamonds, respectively. Solid (dashed, respectively) lines represent positive (negative, respectively) parity levels. The black circles follow the nucleus proton and neutron Fermi levels.

Results similar to the present ones are derived in microscopic approaches using modern versions of the Skyrme force (SkM*, SkP, the SLy and SkI families) [32, 33] and from different versions of the relativistic mean field (RMF) approach [33–35]. However, some parameterizations of the meson Lagrangian yield a $Z = 120$ shell closure much larger than the one at $Z = 126$ [33]. These results are interesting since the magnitude of the spin-orbit two-body force, which determines level ordering in heavy nuclei, is not independent of the other components of the nucleon–nucleon effective interaction in RMF approaches, contrary to non-relativistic descriptions.

In what concerns the deformed shell closures first predicted in [17], practically all approaches, either macroscopic–microscopic or microscopic, find one at $N = 162$, the proton counterpart being $Z = 108$ [32] or $Z = 110$ [13]. Some of them [17], including ours, also find a weaker deformed closure at $N = 152$.

This can be seen in Fig. 2 which displays the single particle energies obtained near the Fermi surface in $^{270}$Hs as a function of $\beta$-deformation. These spectra have been derived by diagonalizing the Hamiltonian $h$ of Eq. (3) calculated with the Gogny force. One can clearly see a large gap at $N = 162$ in the neutron spectrum for $\beta \simeq 0.25$ and smaller one at $N = 152$. In the proton spectrum, $Z = 108$ and $Z = 104$ are subshells at the same deformation. Some of the spherical closures mentioned above also appear in this figure. Let us mention that the existence of these deformed shells is supported by experimental measurements [36].

### *3.2. Deformation properties*

In order to explore ground state and deformation properties, constrained HFB calculations restricted to axial and left–right symmetries have been made for about one hundred even–even nuclei between $Z = 104$ and $Z = 144$, using a constraint on the mass quadrupole moment $Q_{20} = \langle 2r^2 P_2 \rangle$. The PESs obtained in this way have been found to depend essentially on the nucleus neutron number $N$. A representative sample of them is shown in Fig. (3). For $N \simeq 162$ the ground state well is strongly deformed, an effect of the above mentioned $N = 162$ deformed shell, and the fission barrier contains only one hump. As $N$ increases, the ground state deformation decreases gradually and a first hump in the fission barrier develops while the former one progressively disappears. For $N \simeq 184$–188, ground states are spherical and fission barriers reach 10 MeV.

Beyond $N = 190$, the single humped barrier tends itself to vanish. As a consequence, for $N \simeq 192 - 202$, an equilibrium configuration of the nucleus can hardly been found, and the corresponding nuclei should have an extremely short lifetime. However, for larger values of $N$, one observes the birth of a new minimum at large oblate deformation corresponding to $\beta = -0.4$. With respect to the top of the fission barrier, the depth of this oblate minimum reaches 8 MeV for $Z = 128$. A further analysis of this phenomenon showed that this minimum was even much more pronounced for heavier nuclei, in particular those lying on the proton-rich side of the $\beta$-stability line. In $^{360}144_{216}$ for instance, the oblate well is 16 MeV deep and its deformation is $\beta = -0.8$. Unfortunately, calculations performed in triaxial symmetry have shown that the barrier preventing these nuclei to fission is strongly reduced when $\gamma$-deformations are taken into account. For instance in $^{332}124_{208}$, the 6.5 MeV high axial fission barrier is reduced

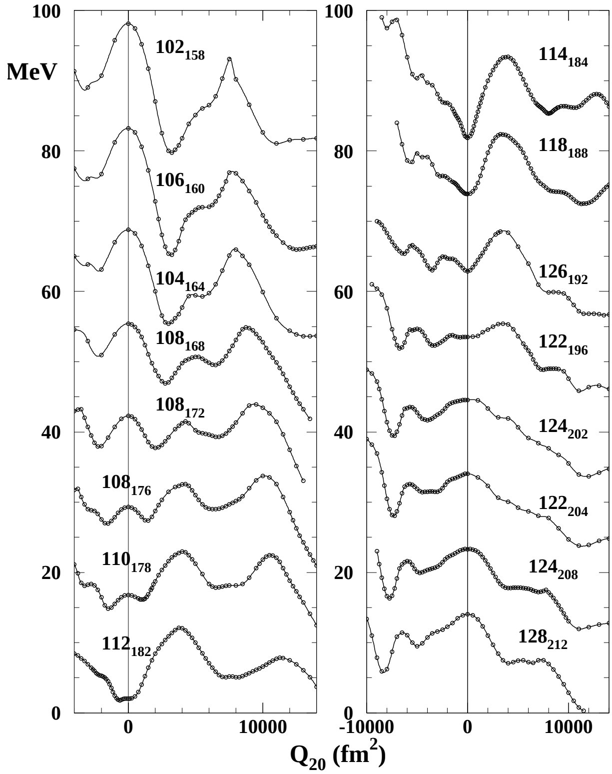


Fig. 3. Deformation energies of a representative set of superheavy nuclei along the line of $\beta$-stability derived from constrained HFB calculations with the Gogny D1S interaction. Axial and left–right symmetries have been imposed. The abscissa is the total axial quadrupole moment $\langle 2r^2P_2\rangle$.

to 2 MeV when triaxial shapes are included. The same kind of calculation performed in $^{360}144_{216}$ shows that the 16 MeV high axial fission barrier is reduced to a very small value, of the order of 100 keV. Although this analysis has not been performed for all nuclei displaying a strongly oblate ground state, it can be expected that most of them have a rather short spontaneous fission half-life.

Ground state $\beta$-deformations for superheavy nuclei with proton numbers $Z$ between 102 and 142 are displayed in Fig. 4. One clearly distinguishes the three regions depending on neutron number discussed above. The transition between prolate deformed nuclei with $N \leq 176$ and spherical ones for $182 \leq Z \leq 192$ is less sharp than the one between spherical nuclei and oblate ones. This is due to shape coexistence between oblate and prolate configurations, as can be seen for instance for $^{280}108_{172}$ in Fig. 3. In this case, the $\beta$ value plotted in the figure is the "dynamical" $\beta$-deformation mentioned at the end of Sec. 2.

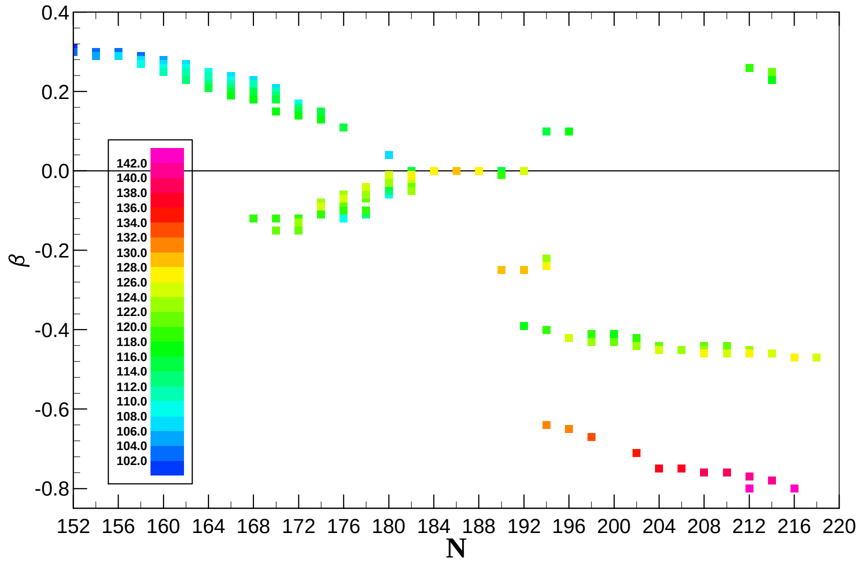


Fig. 4. Ground state $\beta$-deformation of superheavy nuclei as a function of neutron number $N$. The different symbols indicate values of the proton number $Z$ according to the color/grey scale on the left.

For $N > 190$, two lines appear at $\beta = -0.4$ and $\beta = -0.8$ for nuclei having $Z = 118$ to 128 and $Z = 130$ to 142, respectively. They correspond to the nuclei with large oblate ground state deformation mentioned previously. As was discussed, unless particular shell effects develop in some of them, it is unlikely that these nuclei possess a reasonably long lifetime against spontaneous fission.

Let us stress that non-axial deformations and reflection asymmetry usually strongly affect the shape and height of the barriers shown in Fig. 3. Calculations with these symmetries broken have been made for a few nuclei. We find that the high axial fission barrier of $^{298}114$ is not lowered when more general deformations are included. As a consequence, the calculated spontaneous fission half-life $T_{1/2}$ (SF) of this nucleus is larger than $10^9$ years. A different situation is found in the well-known $^{266}$Sg. The one-humped fission barrier displayed in Fig. 3 ($106_{160}$) is found to be unstable against both non-axial and left–right-asymmetric deformations. Taking these deformations into account reduces the fission barrier by 5 MeV, which leads to a decrease of $T_{1/2}$ (SF) from 14 y to 71 s. This time is of the same order of magnitude as the $\alpha$-decay half-life calculated for this nucleus with the model mentioned in Sec. 2, which yields $T_{1/2}(\alpha) = 270$ s (see next section).

These numbers appear in reasonable agreement with experiment: assuming a SF branch of 50% gives 56 s for the calculated half-life of $^{266}$Sg, whereas the measured one is 20 s [36].

This result is a first indication that, at least in calculations with the Gogny force, axial symmetry may lead to a large overestimation of SHE fission barrier heights and fission lifetimes. One must point out in this respect the extensive analysis performed by the Warsaw group [12] who showed that, within macroscopic–microscopic methods, non-axial shapes often lower fission barriers, but do not lead to a decrease in fission half-lives when WKB tunnelling is applied along dynamical fission paths. As such paths minimize the WKB action by including the variations of the nuclear inertia, they are often found to differ significantly from minimum energy paths. This interesting effect is presently being studied in the context of the present microscopic approach.

In even–even nuclei, $Q_\alpha$ are calculated from mass differences for ground state to ground state transitions. In odd and odd–odd nuclei, unique values of $Q_\alpha$'s cannot be unambiguously given since the density of low-lying levels is large and therefore, several allowed transitions may exist. In this case, only the most probable $\alpha$-decay chains will be discussed.

#### 3.2.1. Systematics in even–even nuclei

A systematics of $Q_\alpha$ obtained with the present approach in even–even nuclei between $Z = 102$ and 126 is presented in Fig. 5. The observed $N$-dependence clearly reflects the presence of neutron shells at $N = 162$ (deformed) and $N = 184$ (spherical). Theoretical values appear in fair agreement with experimental data, although $Q_\alpha$'s are slightly underestimated in $Z = 102$ and $Z = 104$ isotopes. One origin of this disagreement may be an overestimation of ground state $\beta$-deformations in these isotopes and a not very pronounced $N = 152$ deformed shell, as compared to macroscopic–microscopic calculations of Refs. [13] and [12] for instance.

The empirical model mentioned in Sec. 2 has been used to compute corresponding $\alpha$-decay half-lives. The result is displayed in Fig. 6. Three regions of increased $\alpha$-decay stability are observed, around neutron numbers 162, 180–188 and 202–212, respectively. These regions correspond to strongly prolate, spherical and strongly oblate nuclei (see Fig. 4). They are clearly related to shell effects in the $Q_\alpha$'s. Let us mention that, due to extreme sensitivity to values of $Q_\alpha$, the uncertainty in the plotted lifetimes can reach two to three orders of magnitude. Still, many nuclei are seen to have $\alpha$ half-lives in excess of 1 s.

A detailed comparison between experimental and theoretical $Q_\alpha$'s for even–even isotopes of nuclei from Cf to $Z = 110$ and for one $Z = 114$ decay chain is shown in Fig. 7. The theoretical results shown have been

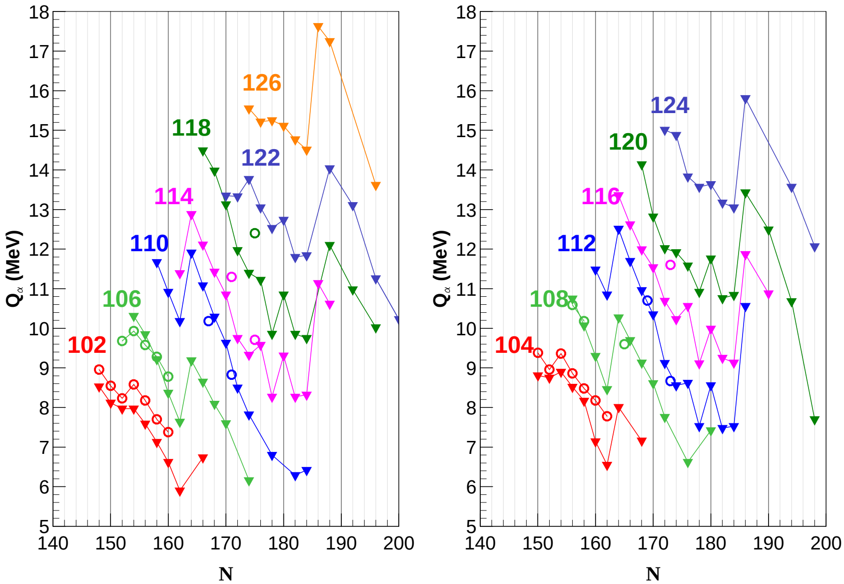


Fig. 5. Theoretical $Q_\alpha$'s deduced from HFB with the Gogny D1S interaction (triangles) compared with available experimental data (circles) for even–even nuclei between $Z = 102$ and 126. The abscissa is the neutron number.

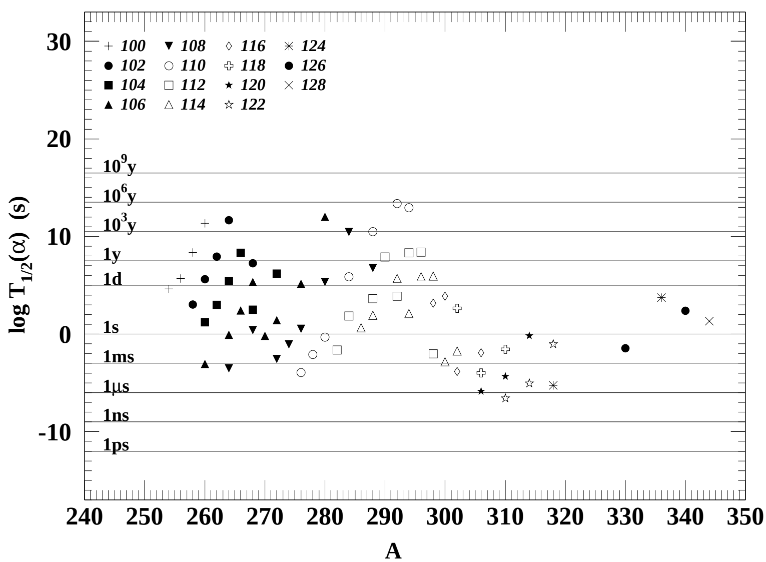


Fig. 6. $\alpha$-decay half-lives calculated from the $Q_\alpha$ of Fig. (5) using the semi-empirical formula of Ref. [29]. The abscissa is the nucleus mass number and the different symbols indicate the proton number $Z$ according to the chart in the top left corner.

obtained from HFB with the Gogny interaction and from the Dirac–Hartree–Bogoliubov (DHB) approach of Ref. [34]. $Q_\alpha$ values are calculated assuming ground state to ground state decay. The Gogny and DHB results appear of similar quality, except for a few isotopes where the two approaches differ by 700 keV to 1 MeV. The DHB method shows the same discrepancy with data in $Z = 102$ isotopes as the HFB Gogny method, but gives a better description of $Q_\alpha$'s in $Z = 104$ ones. This result may be an indication that the relativistic approach employed yields more realistic $\beta$-deformation values in these nuclei than non-relativistic HFB.

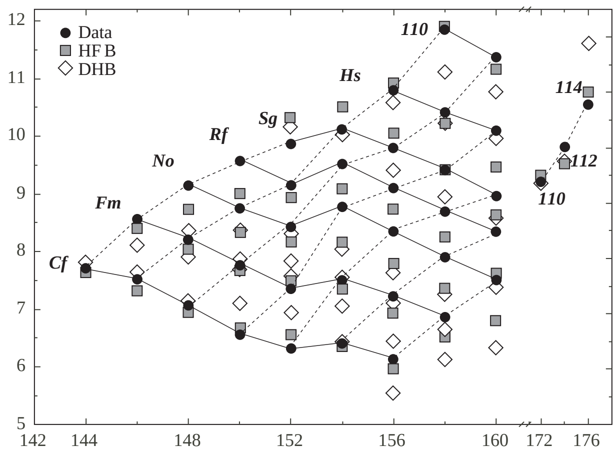


Fig. 7. Theoretical $Q_\alpha$ in MeV obtained from HFB with the Gogny interaction (squares) and from the Dirac–Hartree–Bogoliubov approach of Ref. [34] (diamonds) compared with experimental data (black circles) for even–even nuclei between $Z = 98$ and 114. Isotopes are connected by solid lines whereas dotted lines follow $\alpha$-decay chains. The abscissa is the neutron number $N$.

### 3.2.2. Analysis of odd $Z = 112$ and $Z = 114$ $\alpha$-decay chains

Most available experimental data in the superheavy mass region correspond to odd nuclei. Analysis of the $\alpha$-decay of such nuclei is complicated since ground state to ground state $\alpha$ transitions are often hindered because of parity and angular momentum selection rules. Therefore, all probable decays to low-lying nuclear levels and combinations with possible $\gamma$-ray transitions in daughter nuclei have to be taken into account. Additional effects can also arise from differences in the $\beta$-deformations of the initial and final states in the mother and daughter nuclei. This variety of effects will not be envisaged in detail here. Only a preliminary study of the $\alpha$-decay chains of $^{277}112$ and $^{289}114$ ending with $^{253}$Fm and $^{277}$Hs, respectively, and of the $\alpha$-decay of $^{287}114$ is given in this section.

The $\alpha$-decay chain

$$^{277}112 \xrightarrow{11.45,\,11.17\ \mathrm{MeV}} {}^{273}110 \xrightarrow{11.20,\,11.08\ \mathrm{MeV}} {}^{269}\mathrm{Hs} \xrightarrow{9.23,\,9.18\ \mathrm{MeV}} {}^{265}\mathrm{Sg}$$
$$\xrightarrow{8.62,\,8.75\ \mathrm{MeV}} {}^{261}\mathrm{Rf} \xrightarrow{8.52\ \mathrm{MeV}} {}^{257}\mathrm{No} \xrightarrow{8.34\ \mathrm{MeV}} {}^{253}\mathrm{Fm}\,,$$

where the numbers above the arrows indicate experimentally measured $\alpha$ energies, was first observed at GSI in 1996 [37]. Very recently a new experiment has been performed that confirmed previous results [4]. The time-of-flight of the compound nucleus formed from the reaction $^{70}\mathrm{Zn} + {}^{208}\mathrm{Pb} \rightarrow {}^{278}112$ is in the $\mu s$ range. This is considered long enough for the compound nucleus to be in its ground state before its implantation into the detection system. Therefore, we will assume here that the initial $^{277}112$ is in its ground state.

Fig. 8 displays the low-lying levels calculated with the Gogny force and the HFB blocking technique in axial symmetry for the seven nuclei of the above $\alpha$-decay chain. All possible one-quasiparticle excitations up to 1.0 MeV have been considered. The eigenvalue $K$ of $J_z$ and the parity of excited states is indicated on the left of each level. These nuclei all are prolate in their ground state, with a $\beta$-deformation increasing along the chain from $\beta_2 = 0.12$ in $^{277}112$ to $\beta_2 = 0.30$ in $^{253}$Fm.

In order to examine possible $\alpha$-decay paths, we assume that *(i)* $\alpha$ transitions conserve parity and *(ii)* $\gamma$-ray or internal conversion to lower levels in the daughter nucleus can take place before the next $\alpha$ transition occurs. Let us note that the latter assumption is invalid when the levels populated by $\alpha$

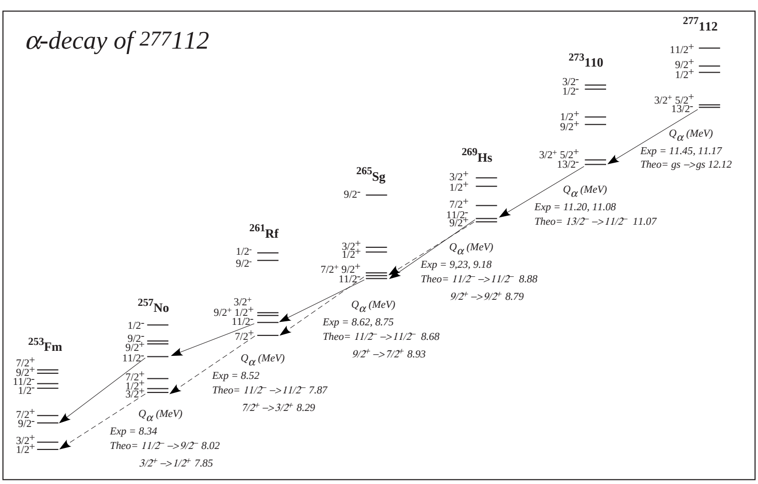


Fig. 8. Calculated levels of the seven nuclei involved in the experimentally observed $\alpha$-decay chain of $^{277}112$. The solid and dashed arrows indicate two positive and negative parity possible paths.

transition are long-lived isomers. The possible positive parity and negative parity paths obtained under these assumptions are shown in Fig. 8 as solid and dashed arrows, respectively.

The decay sequence corresponding to solid arrows can be summarized as follows:

$$
\begin{aligned}
&[716]_{13/2^-}\ {}^{277}112 \overset{12.12\ \mathrm{MeV}}{\longrightarrow} [716]_{13/2^-}\ {}^{273}110 \overset{11.02\mathrm{MeV}}{\longrightarrow} [725]_{11/2^-}\ {}^{269}\mathrm{Hs}\,,\\
&[604]_{9/2^+}\ {}^{269}\mathrm{Hs} \overset{8.79\ \mathrm{MeV}}{\longrightarrow} [604]_{9/2^+}\ {}^{265}\mathrm{Sg}\,,\\
&[725]_{11/2^-}\ {}^{265}\mathrm{Sg} \overset{8.68\ \mathrm{MeV}}{\longrightarrow} [725]_{11/2^-}\ {}^{261}\mathrm{Rf}\,,\\
&[624]_{7/2^+}\ {}^{261}\mathrm{Rf} \overset{8.29\ \mathrm{MeV}}{\longrightarrow} [611]_{3/2^+}\ {}^{257}\mathrm{No} \overset{7.85\ \mathrm{MeV}}{\longrightarrow} [631]_{1/2^+}\ {}^{253}\mathrm{Fm}\,.
\end{aligned}
$$

Excited states are labeled by their Nilsson quantum numbers in addition to $K$ and parity and the numbers above the arrows indicate theoretical $\alpha$ energies. The largest discrepancy with experimental data appears in the energy of the first emitted $\alpha$, where the theoretical result overestimates the experimental one by 670 keV. One could have considered a transition from the $[716]_{13/2^-}$ ground state of ${}^{277}112$ to the $[761]_{1/2^-}$ in ${}^{273}110$. This would reduce the $\alpha$ energy to 10.81 MeV, in slightly better agreement with experiment. However, this $\Delta K = 6$ transition seems to be highly improbable.

Let us stress that the predicted ground state spin-parity of ${}^{253}\mathrm{Fm}$ is $J^\pi = 1/2^+$, in agreement with data from systematics [38]. In ${}^{257}\mathrm{No}$, a $3/2^+$ ground state and a $7/2^+$ level at 200 keV excitation energy are found, whereas systematics predict $J^\pi = 7/2^+$ for the ground state of this nucleus.

The next $\alpha$-decay chain we examine here is the one of the nucleus ${}^{289}114$

$$
{}^{289}114 \overset{9.71\ \mathrm{MeV}}{\longrightarrow} {}^{285}112 \overset{8.67\ \mathrm{MeV}}{\longrightarrow} {}^{281}110 \overset{8.83\ \mathrm{MeV}}{\longrightarrow} {}^{277}\mathrm{Hs}\,.
$$

This chain was observed at Dubna through the reaction ${}^{48}\mathrm{Ca} + {}^{244}\mathrm{Pu}$ where the nucleus ${}^{292}114$ was formed after emission of 3 neutrons [2].

The result of our calculations is displayed in Fig. 9. Under the same assumptions as above, the most probable decay chain is the negative parity one indicated by solid arrows:

$$
\begin{aligned}
&[707]_{15/2^-}\ {}^{289}114 \overset{8.85\ \mathrm{MeV}}{\longrightarrow} [707]_{15/2^-}\ {}^{285}112\,,\\
&[600]_{1/2^+}\ {}^{285}112 \overset{8.36\ \mathrm{MeV}}{\longrightarrow} [600]_{1/2^+}\ {}^{281}110 \overset{9.22\ \mathrm{MeV}}{\longrightarrow} [600]_{1/2^+}\ {}^{277}\mathrm{Hs}\,.
\end{aligned}
$$

Another decay path indicated by dashed arrows can be followed if the transition from the $15/2^-$ state to the $1/2^+$ ground state in ${}^{285}112$ is fast enough. Comparison with experimental data shows that our calculation underestimates the energy of the first emitted $\alpha$ by 860 keV. Any other

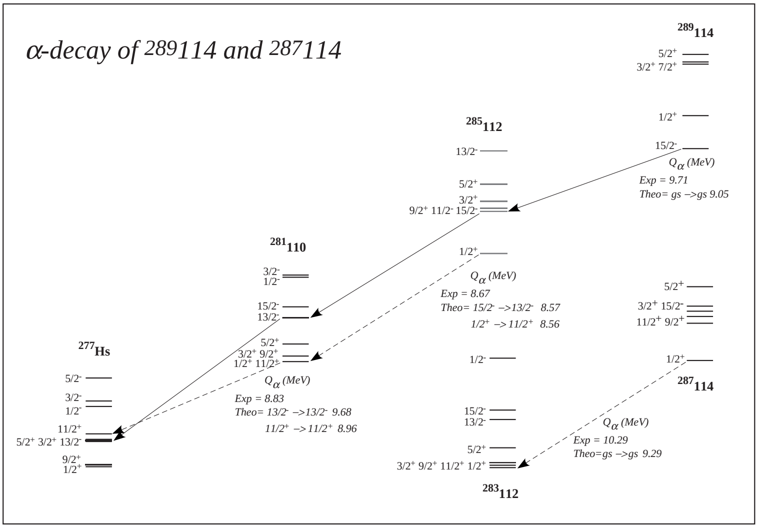


Fig. 9. Calculated levels of the nuclei involved in the experimentally observed $\alpha$-decays chains of $^{289}114$ and $^{287}114$. The solid and dashed arrows indicate negative parity and positive parity possible paths.

possible transition would result in even smaller energies. The energies of the $\alpha$'s emitted by $^{285}112$ and daughter nuclei appear in reasonable agreement with experimental measurements.

Also we give in Fig. 9 a comparison of our result with experimental data for the $\alpha$-decay of $^{287}114$. This nucleus was produced in Dubna in the reaction $^{48}$Ca + $^{242}$Pu [39]. Only one $\alpha$ transition was observed with energy 10.29 MeV before spontaneous fission of $^{283}112$. Here, ground state to ground state transition is the most probable one. In spite of the simplicity of this transition, one observes that our theoretical $Q_\alpha$ underestimates the measured one by 1 MeV. The origin of this discrepancy remains to be determined.

## 4. Conclusion

The study of superheavy nuclei presented in this paper shows that considerable information on the structure and stability of these nuclei can be derived by extending to this domain the microscopic techniques which have proved successful when applied to lighter nuclei. The parameterization of the effective nucleon–nucleon interaction proposed by Gogny appears to yield results in good overall agreement with data for known transactinide nuclei. Still, as we have noticed, discrepancies remain in $Q_\alpha$ values calculated in Nobelium and Rutherfordium isotopes. Also, fission lifetimes computed in the same framework often appear too large. This may be the sign that additional collective degrees of freedom play a role in the description of the deformation properties of these heavy nuclei. Such discrepancies may also originate from the parameterization of specific components of the effective interaction as for instance, the spin-orbit term which is expected to play a crucial role in very heavy nuclei. New developments of relativistic approaches incorporating both exchange terms and pairing correlations in a consistent framework are presently under way [40] whose application to superheavy nuclei would allow one to check this hypothesis and help improve current non relativistic parameterizations of the effective nuclear interaction.

It is an honour and a pleasure for the authors to dedicate this paper to Adam Sobiczewski on the occasion of his 70-th birthday. They are grateful to Brett Carlson and to Klaus Dietrich for many enlightening exchanges and discussions on various topics related to the subject of this paper.

## REFERENCES

[1] M.G. Itkis, Yu.Ts. Oganessian, V.I. Zagrebaev, *Phys. Rev.* **C65**, (2002) 044602.

[2] Yu.Ts. Oganessian *et al.*, *Phys. Rev.* **C64**, 054606 (2001).

[3] V.Yu. Denisov, S. Hofmann, *Phys. Rev.* **C61**, 034606 (2000).

[4] S. Hofmann, G. Münzenberg, *Rev. Mod. Phys.* **72**, 733 (2000); G. Münzenberg, *Nucl. Phys.* **A690**, 175 (2001).

[5] Yu.A. Lazarev *et al.*, *Phys. Rev.* **C54**, 620 (1996).

[6] S. Hofmann, G. Münzenberg, *Rev. Mod. Phys.* **72**, 733 (2000).

[7] S. Hofman *et al.*, *Z. Phys.* **A350**, 277 (1995); *Z. Phys.* **A350**, 281 (1995).

[8] Yu.Ts. Oganessian *et al.*, *Phys. Rev.* **C62**, 041604 (2000).

[9] Yu.Ts. Oganessian *et al.*, *Phys. Rev.* **C63**, 011301(R) (2001).

[10] V.M. Strutinsky, *Yad. Fiz.* **3**, 614 (1966); *Nucl. Phys.* **A95**, 420 (1967); *Nucl. Phys.* **A122**, 1 (1968).

[11] W.D. Myers, W.J. Swiatecki, *Ann. Phys. (N.Y.)* **84**, 186 (1974).

[12] S. Cwiok, A. Sobiczewski, *Z. Phys.* **A342**, 203 (1992); R. Smolańczuk, J.Skalski, H. Klapdor-Kleingrothaus, A. Sobiczewski, *Acta Phys. Pol. B* **24**, 457 (1993); R. Smolańczuk, J. Skalski, A. Sobiczewski, *Phys. Rev.* **C52**, 1871 (1995); A.Sobiczewski, R. Smolańczuk, *Acta Phys. Pol. B* **27**, 1011 (1996); R.A. Gherghescu, Z. Patyk, A. Sobiczewski, *Acta Phys. Pol. B* **28**, 31 (1997); A. Sobiczewski, *Acta Phys. Pol. B* **28**, 21 (1997); *Acta Phys. Pol. B* **29**, 2191 (1998); I. Muntian, Z. Patyk, A. Sobiczewski, *Phys. Rev.* **C60**, 041302 (1999); R.A. Gherghescu, J. Skalski, Z. Patyk, A. Sobiczewski, *Nucl. Phys.* **A651**, 237 (1999); I. Muntian, Z. Patyk, A. Sobiczewski, *Acta Phys. Pol. B* **32**, 691

(2001); I. Muntian, Z. Patyk, A. Sobiczewski, *Phys. Lett.* **B500**, 241 (2001); I. Muntian, A. Sobiczewski, *Acta Phys. Pol. B* **32**, 629 (2001); A. Sobiczewski, I. Muntian, Z. Patyk, *Phys. Rev.* **C63**, 034306 (2001).

[13] P. Möller, J.R. Nix, *Nucl. Phys.* **A549**, 84 (1992); P. Möller, J.R. Nix, *J. Phys. G* **20**, 1681 (1994); P. Möller, J.R. Nix, K.-L. Kratz, *At. Data Nucl. Data Tables* **66**, 131 (1997); P. Möller, J.R. Nix, P. Armbruster, S. Hofmann, G. Münzenberg, *Z. Phys.* **A259**, 251 (1997); P. Möller, A. Iwamoto, *Acta Phys. Hung. N.S.* **10**, 241 (1999).

[14] Z. Lojewski, A. Baran, *Acta Phys. Pol. B* **31**, 485 (2000).

[15] K. Kumar, *Super-Heavy Elements*, IOP Publishing Ltd, Adam Hilger, 1989; *Phys. Scr. T* **32**, 31 (1990); in *Proceedings of the Radioactive Nuclear Beams Third International Conference*, East Lansing, Michigan, May 24–27, 1993, World Scientific.

[16] R.A. Gherghescu, D.N. Poenaru, W. Greiner, *J. Phys. G* **23**, 1715 (1997); *J. Phys. G* **24**, 1149 (1998); *Nuovo Cim.* **A111**, 105 (1998).

[17] Z. Patyk, A. Sobiczewski, *Phys. Lett.* **B256**, 307 (1991); *Nucl. Phys.* **A533**, 132 (1991).

[18] A. Sobiczewski, F.A. Gareev, B.N. Kalinkin, *Phys. Lett.* **22**, 500 (1966); W.D. Myers, W.J. Swiatecki, *Nucl. Phys.* **81**, 1 (1966); C.Y. Wong, *Phys. Lett.* **21**, 688 (1966); H. Meldner, *Ark. Fys.* **36**, 593 (1967); C. Gustafson, I.L. Lamm, B. Nilsson, S.G. Nilsson, *Ark. Fys.* **36**, 613 (1967); S.G. Nilsson, J.R. Nix, A. Sobiczewski, Z. Szymanski, S.Wycech, C. Gustafson, P. Möller, *Nucl. Phys.* **A115**, 545 (1968); S.G. Nilsson, C.F. Tsang, A. Sobiczewski, Z. Szymanski, S. Wycech, C. Gustafson, I.L. Lamm, P. Möller, B. Nilsson, *Nucl. Phys.* **A131**, 1 (1969).

[19] N.N. Bogoliubov, *Sov. Phys. JETP* **7**, 41 (1958); *Sov. Phys. Usp.* **2**, 236 (1959); *Usp. Fiz. Nauk.* **67**, 549 (1959).

[20] J.-F. Berger, K. Pomorski, *Phys. Rev. Lett.* **85**, 30 (2000).

[21] J. Dechargé, D. Gogny, *Phys. Rev.* **C21**, 1568 (1980);

[22] J.F. Berger, M. Girod, D. Gogny, *Comput. Phys. Commun.* **63**, 365 (1991).

[23] J.F. Berger, M. Girod, D. Gogny, *Nucl. Phys.* **A502**, 85c (1989); Z. Patyk, A. Baran, J.F. Berger, J. Dechargé, J. Dobaczewski, P. Ring, A.Sobiczewski, *Phys. Rev.* **C59**, 704 (1999); S. Peru, M. Girod, J.F. Berger, *Eur. Phys. J.* **A9**, 35 (2000); B. Nerlo-Pomorska, K. Pomorski, J.F. Berger, *Acta Phys. Pol. B* **32**, 925 (2001).

[24] J.F. Berger, L. Bitaud, J. Dechargé, M. Girod, K.Dietrich, *Nucl. Phys.* **A685**, 1c (2001).

[25] M. Girod, B. Grammaticos, *Phys. Rev.* **C27**, 2317 (1983).

[26] S.T. Belyaev, *Mat. Fys. Medd. Dan. Vid. Selsk.* **31**, No. 11 (1959); *Nucl. Phys.* **24**, 322 (1961).

[27] P. Ring, P. Schuck, *The Nuclear Many–Body Problem*, Springer–Verlag, New York 1980.

[28] S.G. Nilsson *et al.*, *Nucl. Phys.* **A131**, 1 (1969).

[29] J. Dechargé, L. Pangault, *Rapport CEA-R-5672*, CEA Bruyères-le-Châtel, France, 1994.

[30] J. Dechargé *et al.*, *Phys. Lett.* **B451**, 275 (1999).

[31] S.Ćwiok *et al.*, *Nucl. Phys.* **A611**, 211 (1996); *Phys. Rev. Lett.* **83**, 1108 (1999); A.T. Kruppa *et al.*, *Phys. Rev.* **C61**, 034313 (2000).

[32] S. Cwiok, S. Hofmann, W. Nazarewicz, *Nucl. Phys.* **A573**, 356 (1994).

[33] K. Rutz *et al.*, *Phys. Rev.* **C56**, 238 (1997); M. Bender *et al.*, *Phys. Rev.* **C58**, 2126 (1998); *Phys. Rev.* **C60**, 034304 (1999); T. Bürvenich *et al.*, *Eur. Phys. J.* **A3**, 139 (1998); S.K. Patra, W. Greiner, R.K. Gupta, *J. Phys. (London) G* **26**, L25 (2000).

[34] D. Hirata *et al.*, *Nucl. Phys.* **A616**, 438c (1997); B.V. Carlson, D. Hirata, *Phys. Rev.* **C62**, 054310 (2000).

[35] G.A. Lalazissis, M.M. Sharma, P. Ring, Y.K. Gambhir, *Nucl. Phys.* **A608**, 202 (1996); G.A. Lalazissis, J. Konig, P. Ring, *Phys. Rev.* **C55**, 540 (1997).

[36] Yu. Lazarev *et al.*, *Phys. Rev. Lett.* **73**, 624 (1994).

[37] S. Hofmann *et al.*, *Z. Phys.* **A354**, 229 (1996).

[38] Nuclear wallet cards VI ed., National nuclear data center.

[39] Yu.Ts. Oganessian *et al.*, *Nature (London)* **400**, 242 (1999).

[40] B.V. Carlson, D. Hirata, in preparation.